1. Methods

1.1. Operation Schedule of the Wastewater Pumps

Diurnal hydraulic residence times and operation schedule of the wastewater pumps used for the intermittent and dosing test applications.

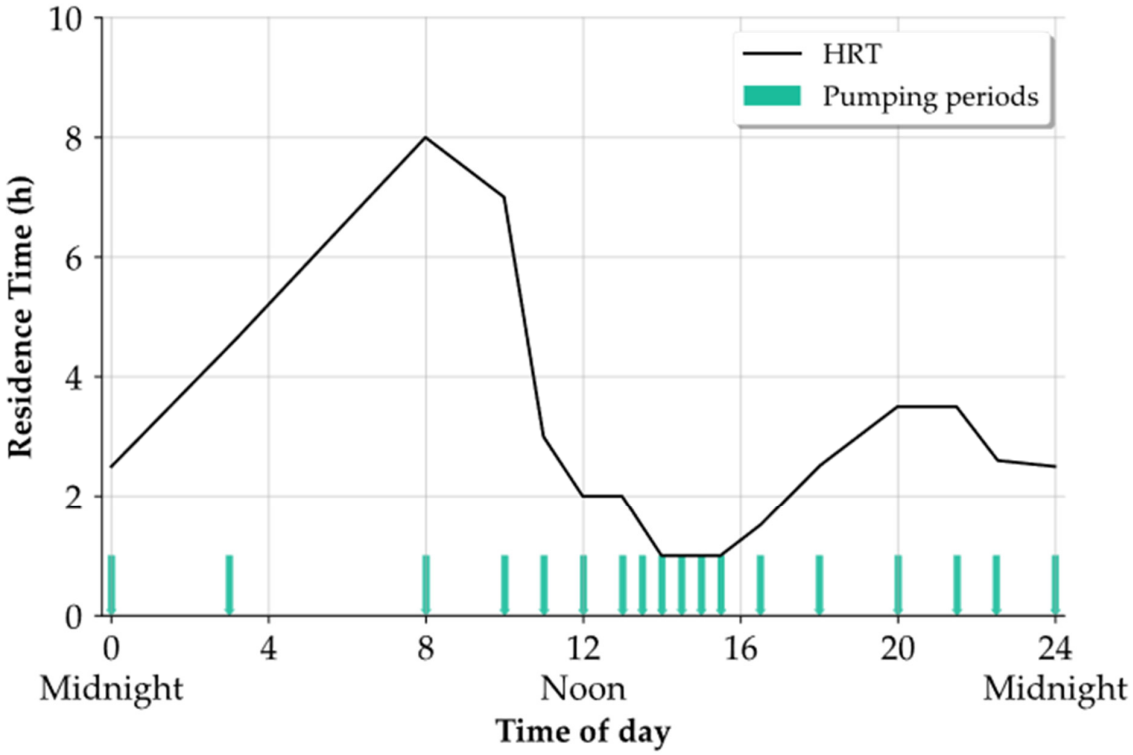

Figure S1. Operation schedule of the wastewater pumps [1]. Diurnal hydraulic residence time curve in (–), Wastewater pumping events are in (▪).

Table S1. Metrics used for comparing sensor data following [2]. M_i indicates H_2S measurements made by the online sensors (ISA, OPUS, SulfiLogger™) compared and RM_i indicates the reference measurements (ECH H_2S Analyzer Cubi).

Comparison Metrics	Short Name	Formula	Characteristics
Mean Bias	MB	$\frac{1}{n}\sum_{i=1}^{n}(RM_i - M_i)$	Estimation of the magnitude of differences between sensors estimation and reference values averaged over the whole sampling period.
Pearson's Correlation Coefficient	r	$\frac{\frac{1}{n}\sum_{i=1}^{n}(M_i - \overline{M})(M_i - \overline{RM})}{\sqrt{\frac{1}{n}\sum_{i=1}^{n}(M_i - \overline{M})^2 \frac{1}{n}\sum_{i=1}^{n}(RM_i - \overline{RM})^2}}$	Measures the strength and the direction of a linear relationship between two variables and receives a value between -1 and 1
Concordance Correlation Coefficient	CCC	$\frac{2S_{MRM}}{S_M^2 + S_{RM}^2 + (\overline{M} - \overline{RM})^2}$	Measures the agreement between the variables x and y by assessing the extent to which they fall on the line of equality. Line of equality defined as the 45° line through the origin [3]. CCC is 1 when all points fall on the line of equality.
Root Mean Square Difference	RMSD	$\sqrt{\frac{1}{n}\sum_{i=1}^{n}(M_i - RM_i)^2}$	Indicates the magnitude of the difference and retains the variable's unit; is sensitive to extreme values and to outliers; tends to vary as a function of the standard deviation of the RM.

Unbiased Root Mean Square Difference	uRMSD	$\sqrt{\frac{1}{n}\sum_{1}^{N}[(M_i-\bar{M})-(RM_i-\overline{RM})]^2}$	Used for the quadratic decomposition of RMSD as the sum of Mean Bias Error and Centered Root Mean Error; is an indicator of the sensor random error. Can be normalized with the standard deviation of the observations from the reference instrument.
Mean Absolute Error (Difference)	MAE	$\frac{1}{n}\sum_{i=1}^{n}\lvert M_i-\mathrm{RM}_i\rvert$	Measures the absolute mean difference between the reference and sensor measurement. Smaller the MAE, the closer the sensor measurements are to reference method
Mean of M:		$\bar{M}=\frac{1}{n}\sum_{i=1}^{n}M_i$	
Variance of M:		$S_M^2=\frac{1}{n}\sum_{i=1}^{n}(M_i-\bar{M})^2$	
Covariance of M and RM		$S_{MRM}=\frac{1}{n}\sum_{i=1}^{n}(M_i-\bar{M})\,(RM_i-\overline{RM})$	

1.2. Bland-Altman plot.

The Bland-Altman (BA) plots are illustrated in Figure 2(e-f) in the manuscript. BA plots are used to describe the agreement between two measurement pairs by constructing limits of agreement [4]. The plot is shown as a scatter plot, in which the Y axis shows the difference between paired measurement $(RM-M)$ and the X axis gives the averaged of these measurements $((RM+M)/2)$ [4]. A key step in the BA anaylsis is to ensure that the differences of the measurement pairs are normally distribtued. Thus, we used to the Shapiro-Wilk test to determine if the distribution is normal. If normally this distributed then most of the differences will lie between $MB-1.96SD$ and $MB+1.96SD$ where SD is the standard deviation of differences. In the BA plots presented in the manuscript, the 95% confidence interval (CI) of the mean bias and agreements were included. For details in the implements the CI bands see [4,5]

1.3. Target diagram

According to [6,7], the target diagram is derived from the relation between the statistical metrics of bias (MB), unbiased root-mean-square difference $(uRMSD)$, and $RMSD$ (Eq. 1). The diagram uses a Cartesian coordinate system where the x-axis represents the $uRMSD$ (variance of the difference), and the y-axis represents MB. Since these three metrics are related by the equation (Equation S1)

$$RMSD^2 = MB^2 + uRMSD^2 \quad \text{(S1)}$$

the distance between any point to the origin is equal to the $RMSD$, contours of which lead to the diagram having the appearance of a common target poster.

1.4. H_2S removal percentages

Calcuation of the H_2S removal percentages using the sensors' measurements obtained during calcium nitrate dosing trials. Baseline monitoring corresponds to the measurements recorded during the intermittent pumping test application.

$$H_2S_{removal}(\%) = \frac{H_2S_{baseline} - H_2S_{nitrate\ dosing}}{H_2S_{baseline}} \times 10 \quad \text{(S2)}$$

2. Results

2.1. Summary of the Comparison Data Set (Phase1)

Table S2. Statistical distribution measures of the reference and sensors H_2S measurements were used for the comparison.

Measurement	Median	MAD	Range
ECH (reference) (H_2S mg L^{-1})	1.90	1.36	0.26 to 16.78 mg/L
ISA (H_2S mg L^{-1})	2.40	1.26	0.91 to 9.18 mg/L
OPUS (H_2S mg L^{-1})	3.95	2.19	0.57 to 21.75 mg/L
SulfiLogger™ (H_2S mg L^{-1})	1.27	0.97	0.10 to 9.73 mg/L
Temperature (°C)	19.5	0.6	13.8 to 20.5 °C
pH (-)	7.4	0.3	6.9 to 8.02

2.2. Summary of the statistical comparison measures applied to the comparison pairs

Table S3. Summary of the statistical comparison measures applied to the comparison pairs.

		r	R^2	CCC	Bias	RMSD	MAE	% of Values in ±1 Range
Dataset	Comparison							
All	ECH-ISA	0.92	0.85	0.82	0.16	2.12	1.30	73%
	ECH-OPUS	0.94	0.88	0.81	-2.48	3.18	2.65	14%
	ECH-SFL	0.87	0.76	0.78	0.70	2.39	1.75	50%
<=5	ECH-ISA	0.74	0.55	0.61	-0.69	1.14	0.79	68%
	ECH-OPUS	0.65	0.43	0.28	-2.11	2.88	2.33	14%
	ECH-SFL	0.10	0.01	0.09	-0.13	1.64	1.23	50%
>5	ECH-ISA	0.89	0.78	0.26	3.07	3.92	3.07	5%
	ECH-OPUS	0.92	0.85	0.59	-3.73	4.03	3.73	0%
	ECH-SFL	0.85	0.72	0.39	3.50	3.99	3.50	0%

2.3. Target diagram

The purpose of the target diagram is to compactly summarize the statistical quantities used to assess the accuracy or skill of the sensor's measurements when compared to the measurement obtained by the reference method (ECH). The target diagram reveals that both ISA and Sulfilogger™ were of relatively similar accuracy, as highlighted by the close grouping in the target diagram. Despite having similar unbiased RMSD values to the ISA and SulfiLogger, the target diagram showed that the mean bias of the OPUS was the main contributor to the total RMSD.

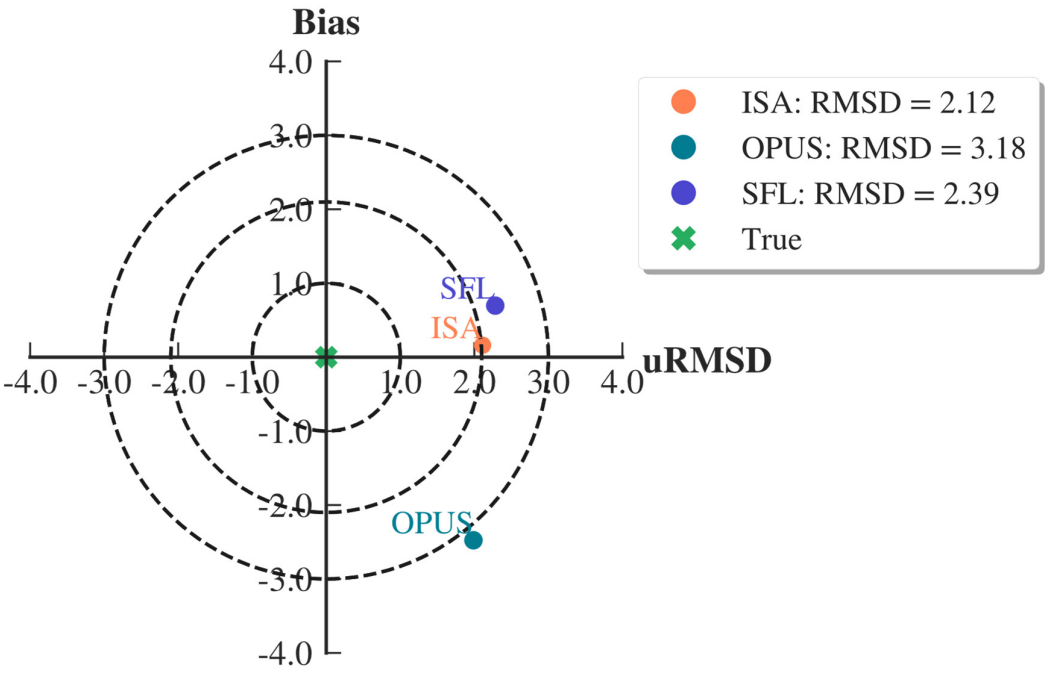

Figure S2. Target diagram for comparing the reference and sensors' measurements. The unbiased RMSD is displayed on the x-axis. The y-axis denotes the bias (the mean difference between the reference and sensor measurement). The true or ideal agreement is highlighted by ✖ the UV/Vis sensor (● ISA), the UV sensor (● OPUS), and the electrochemical sensor (● SLF). The units of the diagram are all expressed in H_2S concentration (mg L^{-1}).

2.4. Summary of the statistical distribution measures of the sensors for test applications (Phase 2)

Table S4. Summary of the statistical distribution measures of the sensors for test applications (Phase 2).

Test application	Sensor	Flow			No flow		
		Median (H_2S mg L^{-1})	*MAD* (H_2S mg L^{-1})	*Range* (H_2S mg L^{-1})	*Median* (H_2S mg L^{-1})	*MAD* (H_2S mg L^{-1})	*Range* (H_2S mg L^{-1})
Intermittent	SLF	5.37	1.29	2.07 - 10.47	5.93	1.30	2.38 - 10.3
	OPUS	6.61	1.78	2.21 - 17.17	6.28	1.81	1.47 - 23.47
	ISA	3.42	0.77	1.39 - 7.04	3.27	0.76	1.14 - 7.74
Constant	SLF	1.66	0.25	1.16 - 4.12			
	OPUS	2.00	0.18	0.02 - 3.84			
	ISA	2.68	0.14	2.36 - 3.72			
Nitrate 7.5 mg-N L^{-1}	SLF	0.82	0.74	0.04 - 4.8	1.94	0.07	0.01 - 8.37
	OPUS	3.02	1.26	0.07 - 11.41	2.47	0.01	0.01 - 12.9
	ISA	3.14	0.83	1.93 - 6.88	3.74	0.06	1.79 - 9.27
Nitrate 14 mg-N L^{-1}	SLF	0.34	0.12	0.08 - 1.41	0.28	1.50	0.02 - 1.27
	OPUS	0.36	0.23	0 - 2.37	0.14	1.48	0 - 1.84
	ISA	2.21	0.31	0.44 - 13.78	2.07	1.30	0.48 - 6.32
Nitrate 28 mg-N L^{-1}	SLF	0.14	0.05	0.01 - 0.52	0.17	0.15	0 - 1.5
	OPUS	0.05	0.02	0 - 0.48	0.01	0.11	0 - 0.29
	ISA	0.00	0.03	0.01 - 0.52	-0.01	0.47	-0.23 - 2.29

2.5. Response of nitrate sensors during flow and no flow periods during nitrate dosing application

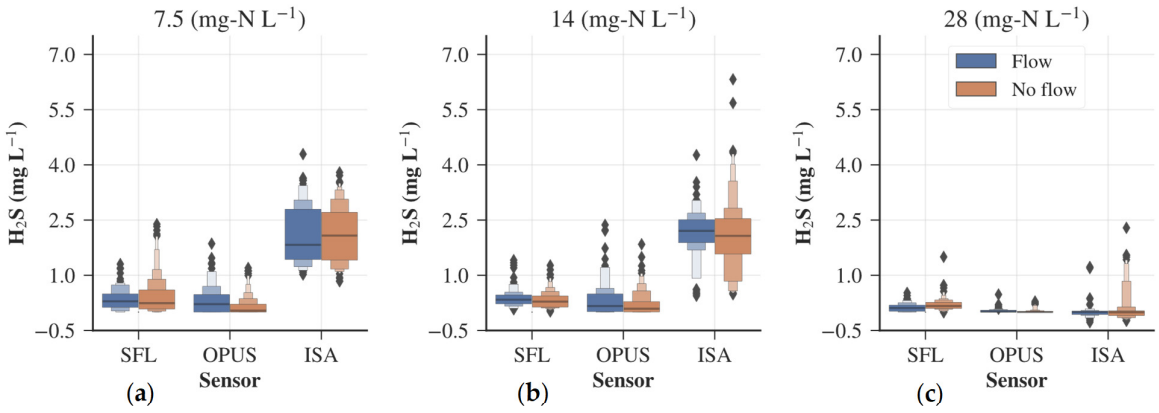

Figure S3. Letter-value plots [8] comparing the H_2S measurements during periods of active mixing (■ pump on) and still conditions (■ pump off) during the dosing scenarios. Limited nitrate dosing - (**a**). Optimal -14 mg/L (**b**). Overdosing 28 mg/L (**c**). Median measurements are represented by the horizontal line segment (—). Identified outliers are represented by(♦). Heavily shaded innermost boxes indicate a higher data density.

2.6. Possible effect of iron salts dosing application on optical sensors

Effects of iron sulfide precipitate produced during the ferric nitrate dosing on the lens of the optical sensors used in this study.

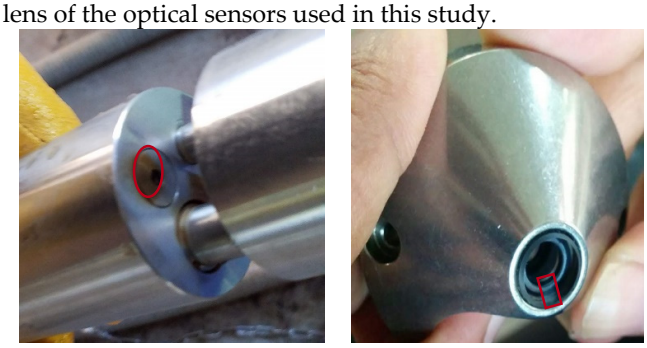

Figure S4. Possible effect of iron salts dosing application on optical sensors. ISA GO (**a**) and TriOS OPUS (**b**) where affected by discolouration and scratching of the lens after one month of Ferric Nitrate dosing.

References

1. Despot, D.; Reinhold, L.; Augustyniak, A.; Barjenbruch, M. Dosing Free Nitrous Acid as an Alternative Sulphide Control Technology for Pressure Sewers in Germany. *Water* **2021**, *13*, 1015, doi:10.3390/w13081015.

2. Borrego, C.; Costa, A.M.; Ginja, J.; Amorim, M.; Coutinho, M.; Karatzas, K.; Sioumis, Th.; Katsifarakis, N.; Konstantinidis, K.; De Vito, S.; et al. Assessment of Air Quality Microsensors versus Reference Methods: The EuNetAir Joint Exercise. *Atmos. Environ.* **2016**, *147*, 246–263, doi:10.1016/j.atmosenv.2016.09.050.

3. Echavarría-Heras, H.; Leal-Ramírez, C.; Villa-Diharce, E.; Castillo, O. Using the Value of Lin's Concordance Correlation Coefficient as a Criterion for Efficient Estimation of Areas of Leaves of Eelgrass from Noisy Digital Images. *Source Code Biol. Med.* **2014**, *9*, doi:10.1186/s13029-014-0029-8.

4. Giavarina, D. Understanding Bland Altman Analysis. *Biochem. Medica* **2015**, *25*, 141–151, doi:10.11613/BM.2015.015.

5. Bland, J.M.; Altman, D.G. Measuring Agreement in Method Comparison Studies. *Stat. Methods Med. Res.* **1999**, *8*, 135–160, doi:10.1177/096228029900800204.

6. Jolliff, J.K.; Kindle, J.C.; Shulman, I.; Penta, B.; Friedrichs, M.A.M.; Helber, R.; Arnone, R.A. Summary Diagrams for Coupled Hydrodynamic-Ecosystem Model Skill Assessment. *J. Mar. Syst.* **2009**, *76*, 64–82, doi:10.1016/j.jmarsys.2008.05.014.
7. Rochford, P. *PeterRochford/SkillMetrics*; 2021;
8. Hofmann, H.; Wickham, H.; Kafadar, K. Letter-Value Plots: Boxplots for Large Data. *J. Comput. Graph. Stat.* **2017**, *26*, 469–477, doi:10.1080/10618600.2017.1305277.